

Lateral Diffusion in Planar Lipid Bilayers: A Fluorescence Recovery after Photobleaching Investigation of Its Modulation by Lipid Composition, Cholesterol, or Alamethicin Content and Divalent Cations

S. Ladha,* A. R. Mackie,* L. J. Harvey,* D. C. Clark,* E. J. A. Lea,* M. Brullemans,[§] and H. Duclouhier[§]

*Institute of Food Research and *University of East Anglia, Norwich, NR4 7UA England, and [§]URA 500 CNRS-Université de Rouen, 76821 Mont-Saint-Aignan, France

ABSTRACT In spite of the fact that planar lipid bilayers are still the best-suited artificial membrane system for the study of reconstituted ion channels and receptors, data dealing with their physical characterization, especially as regards dynamics, are scanty. A combined electrical and optical chamber was designed and allowed fluorescence recovery after photobleaching recovery curves to be recorded from stable virtually solvent-free bilayers. *D*, the lateral diffusion coefficient of *N*-(7-nitrobenzoyl-2-oxa-1,3-diazol-4-yl)-1,2-dihexadecanoyl-sn-glycero-3-phosphoethanolamine, was found to be relatively insensitive to the phospholipid composition (headgroup, chain unsaturation, etc.), whereas inclusion of 33–50% cholesterol in the membrane reduced *D* by a factor of 2. Divalent cations significantly reduced *D* of negatively charged bilayers. These results compare well with data gathered on other model and natural systems. In addition, the incorporation of the voltage-dependent pore-former alamethicin did slightly reduce lipid lateral mobility. This study demonstrates the feasibility of such experiments with planar bilayers, which are amenable to physical constraints, and thus offers new opportunities for systematic studies of structure-function relationships in membrane-associating molecules.

INTRODUCTION

The dynamics of molecules in membranes (order parameter, degree of freedom of lipid aliphatic chains, lateral and rotational diffusions), often referred to as membrane fluidity, has been associated with modulation of the activity of many important functions of proteins in biological membranes (for a review, see Shinitzky, 1984a). After cold or heat adaptation and diet changes, the membrane lipid composition can readjust via metabolic pathways so as to provide an optimal lipid environment (the “homeoviscous theory”; see, e.g., Cossins, 1983; Cuculescu et al., 1995). Alterations in the microviscosity (and presumably the lateral mobility) can also be strongly correlated to some pathologies (Shinitzky, 1984b). Lateral diffusion within natural or artificial membranes is one of the most well-characterized parameters related to the dynamic state of the membrane (see review by Tocanne et al., 1994). It has fundamental implications for functional coupling between membrane components through collisional mechanisms as, for example, in the photosynthetic electron chains (Blackwell et al., 1994), in visual transduction (Lamb, 1994), as well as in receptor-mediated endocytosis (Schlessinger, 1993) and intercellular adhesion (Leckband et al., 1992). Recently, new techniques such as “single particle tracking” demonstrate that lateral diffusion is not homogeneous throughout the plasma membrane of most cells (Anderson et

al., 1992; Cherry et al., 1994; Jacobson et al., 1995). Specific examples include cell junctions of vascular endothelium (Tournier et al., 1989) and neurons (Joe and Angelides, 1993).

Fluorescence recovery after photobleaching (FRAP) has become, over the last 15 years, the most direct and elegant way of measuring the rate of lipid and protein lateral diffusion, mostly within biological membranes such as red blood cells (Bloom and Webb, 1983). Significant theoretical and methodological improvements, such as the “fringe or periodic pattern bleaching” (Smith and McConnell, 1978), later improved by Davoust et al. (1982), and more recently “scanning microphotolysis” (Wedekind et al., 1994), complement the basic technique.

Although most spectroscopic investigations dealing with membrane models have been carried out on populations of lipid vesicles, planar lipid bilayers have become popular model systems for characterizing the function of purified voltage-gated channels, receptors and their peptide models (see, e.g., Krueger et al., 1983; Hanke and Schlue, 1993; Chang et al., 1995). Pioneering work on direct measurement of the lateral diffusion coefficient (*D*) of fluorescent probes in lipid bilayers was carried out with bilayers supported on a circular platinum loop (Koppel et al., 1976) and on electron microscopy grids (Fahey and Webb, 1978). However, little effort has since been devoted to characterizing *D* in more “realistic” model membranes used in reconstitution studies. The present work gives the first determinations of *D* on “virtually solvent-free” Montal-Mueller bilayers (referred to hereafter as PLB for planar lipid bilayers) formed in a conventional manner (Montal and Mueller, 1972), which are amenable to simultaneous fluorescence recovery after photobleaching (FRAP) as well as conductance experiments.

Received for publication 31 October 1995 and in final form 22 May 1996.

Address reprint requests to Dr S. Ladha, Institute of Food Research, Norwich Science Park, Colney Lane, Norwich NR4 7UA England. Tel.: 44-1-603-255000 Fax: 44-1-603-507723; E-mail: ladhas@bbsrc.ac.uk.

Dr. Brullemans' present address is Sciencetech International, 3521 rue de Courval, Trois-Rivières, G8Z-1S8 Québec, Canada.

© 1996 by the Biophysical Society

0006-3495/96/09/1364/10 \$2.00

MATERIALS AND METHODS

Materials

The lipids 1-palmitoyl-2-oleoyl-sn-glycero-3-phosphocholine (POPC), 1,2-dioleoyl-sn-glycero-3-phosphocholine (DOPC), 1,2-dioleoyl-sn-glycero-3-phosphoethanolamine (DOPE), and 1,2-dioleoyl-sn-glycero-3-phospho-L-serine (DOPS) were purchased from Avanti Polar Lipids (Birmingham, AL) and used without further purification. Cholesterol (CHOL) was purchased from Sigma Chemical Company (St. Louis, MO). The fluorophore *N*-(7-nitrobenzoyl-2-oxa-1,3-diazol-4-yl)-1,2-dihexadecanoyl-sn-glycero-3-phosphoethanolamine (NBD-PE) was purchased from Molecular Probes (Eugene, OR).

Virtually solvent-free planar lipid bilayer formation

A 25- μm -thick PTFE septum (Goodfellow, Cambridge, England) with a hole of 200–300- μm diameter (made by an electric arc discharge) in the center was clamped into a specially designed chamber, allowing simultaneous electrical (conductance and capacitance) and FRAP measurements (Fig. 1). The body of the cell was machined from two blocks of polytetrafluoroethylene (PTFE). The cell was assembled by carefully positioning the PTFE septum between the cell halves with the hole located centrally. Optical windows were fitted in the recesses of the outer faces of the cell. These in turn were held in position by a temperature-controlled brass housing that was clamped against each face of the cell. Before membrane formation, the hole in the septum was coated with 1 μl of 1% (v/v) hexadecane in hexane on each side. The hexane was allowed to evaporate. To form Montal and Mueller bilayers, buffer (100 mM or 1 M KCl, 1 mM HEPES, pH 7.4) was added to each side of the chamber such that the level was above the hole in the septum. Lipid containing 1 mol% NBD-PE was spread from a hexane-ethanol (9:1 v/v) solution on the buffer surface in the

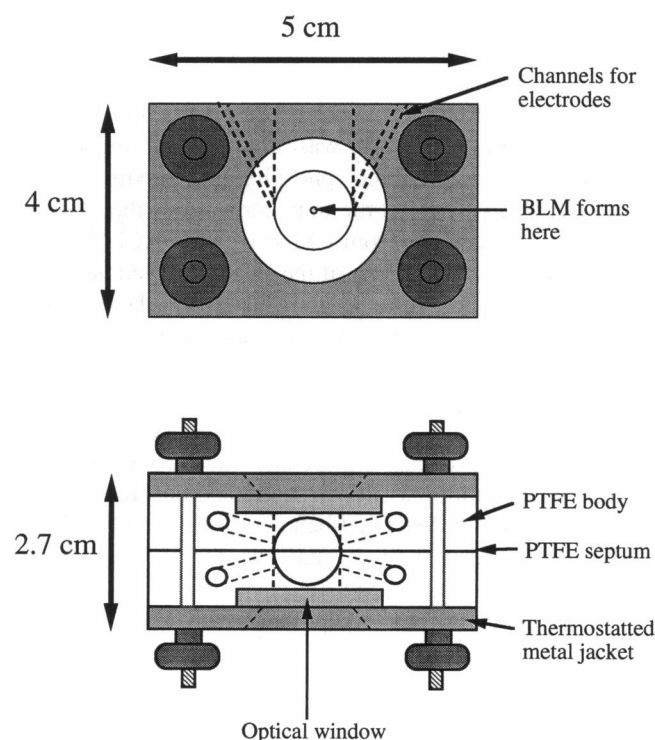


FIGURE 1 A schematic diagram of the cell developed for formation of planar lipid bilayers (PLBs) for combined optical and electrical measurements.

chambers and allowed to stand for a few minutes to allow evaporation of the solvent. The buffer level on the *trans* side was lowered below the hole in the PTFE septum and then raised back to its original level. PLB formation was monitored visually and by capacitance measurements.

Capacitance and conductance measurements

Conductance and capacitance measurements were performed from the same experimental set-up. A DC voltage or a mixed DC-AC voltage from a signal generator (20 MHz pulse/function generator, model 628; Dynatech) is applied in the *cis* side of the bilayer via Ag/AgCl electrode. A second Ag/AgCl *trans* electrode is connected to an *I-V* converter (RAP Montgomery, model HAMK2; London) with a 1-G Ω feedback resistor. The output signal is then filtered by a dual variable filter (Kemo, model VBF4; Beckenham, England) and sent to an oscilloscope, an X-Y recorder, or a microcomputer. For the conductance measurements, a DC or a low-frequency (0.01 Hz) triangular voltage is applied to ensure steady-state instantaneous current responses. For capacitance measurements, a triangular wave of high frequency (amplitude 10 mV, frequency 100 Hz) was applied to the bilayer. If the conductance of the bilayer remains low, the capacitance of the system can be directly obtained from the rms value of the squared output ($I = C \, dV/dt$), capacitance being equal to V/K , with $K = 10 \, \text{mV} \cdot \text{pF}^{-1}$. The system was calibrated with capacitors of known values, and the contribution of the line (cables, connections, etc., outside the bilayer) was subtracted.

Fluorescence recovery after photobleaching

Measurement of the lateral diffusion coefficient of the fluorophore NBD-PE in planar lipid bilayers was achieved using the FRAP method. A schematic diagram of the apparatus is shown in Fig. 2 and was developed from our conventional spot photobleaching FRAP set-ups that are based on upright (Ladha et al., 1994) and inverted (Clark et al., 1990) microscopes. Essentially the apparatus was constructed using components from a Nikon Optiphot microscope mounted on its side (i.e., with a horizontal optical axis). The nosepiece and binocular eyepiece of the microscope were

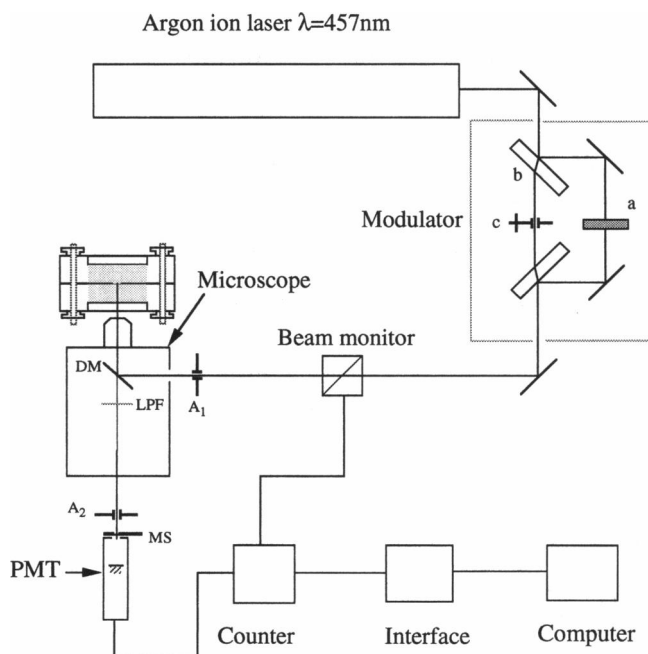


FIGURE 2 Schematic diagram of the principal components of the fluorescence recovery after photobleaching (FRAP) apparatus.

mounted on a special Nikon bracket, which was bolted to an optical rail (Newport, Microcontrol) on the laser table (Photon Control, Cambridge). The PLB cell was mounted on a separate bracket attached to a micrometer-controlled translation stage to allow focusing, and the stage was again bolted to the optical rail.

The intensity of the 457-nm beam of a 10-W argon ion laser (Innova 100-10) was attenuated by reflection off glass flats and by passing through a neutral density filter, as shown in Fig. 2. When the fast electronic shutter (Uniblitz) (c) is closed, only the monitoring laser beam (a) illuminates the sample. When the shutter is open the intense, bleaching beam (b), which is transmitted through two of the glass flats, passes through to the sample. The beam provided by the modulator (Coherent Innova, model 304A) passes through a beam monitor (beam splitter and photodiode), the signal from which is used to electronically compensate for minor fluctuations in the laser beam intensity. The laser beam then passes through a pinhole aperture (A_1) located at the image plane, at the entrance port of the epiillumination attachment of the fluorescence microscope. A 510-nm dichroic mirror (DM) and a 500-nm long-pass filter (LPF) were used to ensure that only emitted light reached the photon counting photomultiplier tube (PMT) (Thorn-EMI 9816B) positioned at the camera port of the binocular eyepiece. The PMT was protected during the bleaching pulse by an electronic gating circuit and a mechanical shutter (MS). Before entering the detector, the emitted light beam passed through a second aperture (A_2), again positioned at the image plane. The laser beam profile and spot radius at the point of focus were determined by using a beam scanner (BeamScan model 2180; Photon, Inc.). The laser beam was of Gaussian cross-sectional intensity, with a half-width at $1/e^2$ height of the laser beam at its point of focus equal to $3.3 \mu\text{m}$ (spot radius). System timing and control, data acquisition, and data analysis were performed with a VME microcomputer system (Motorola 68020). The microscope and cell were enclosed with an aluminium box, which acted as a Faraday cage and minimized noise in the conductance measurements.

All FRAP experiments were performed at a controlled room temperature of 23°C . The laser spot (spot radius $3.3 \mu\text{m}$) was directed at the center of the PLB and was sufficiently small for the surrounding bilayer to act as a near infinite reservoir. In the experiments described below, generally 10 FRAP curves were collected for each set of conditions and averaged before analysis. FRAP data were analyzed by nonlinear least-squares fitting to an expression defining the time dependence of fluorescence recovery observed with a circular beam of Gaussian cross-sectional intensity and had the form (Yguerabide et al., 1982)

$$F(t) = \frac{F(0) + F(\infty)(t/\beta\tau_D)}{1 + (t/\beta\tau_D)},$$

where $F(t)$ is the observed fluorescence as a function of time, $F(0)$ is the intensity of the fluorescence immediately after the bleach pulse, $F(\infty)$ is the fluorescence at infinite time after the bleach pulse, β is the depth of bleach parameter (Clark, 1995), and τ_D is the characteristic diffusion time. The lateral diffusion coefficient, D , is given by $D = \omega^2/4\tau_D$, where ω (spot radius) is the half-width at $1/e^2$ height of the laser beam at its point of focus on the membrane. The percentage mobile fraction (%R; percent recovery) is given by

$$\%R = \frac{F(\infty) - F(0)}{F(t < 0) - F(0)},$$

where $F(t < 0)$ is the prebleach fluorescence (Wolf, 1989).

RESULTS

Capacitance and lateral diffusion characteristics of the bilayers

Once the bilayer was formed, continuous monitoring of membrane capacitance revealed either a gradual or rapid approach to a steady-state value (Fig. 3, A and B, respec-

tively). Even when the approach was gradual, reflecting the slow evaporation of residual solvent (Vodyanoy and Murphy, 1982), it was complete within a relatively short time. In the worst case, the process was complete within 12 min. The lifetime of the bilayer was typically 2 h, which allowed many determinations (every 2–3 min) of the D , the lateral diffusion coefficient of NBD-PE.

The recovery portion of a typical, averaged FRAP data curve from a virtually solvent-free PLB formed from DOPC containing 1% NBD-PE is shown in Fig. 4. The computed best fit to the curve obtained is also shown, along with the residuals (experimental curve – computed fit). The fit returned a τ_D value of 179 ± 15 ms, which converts to a lateral diffusion coefficient of $15.2 \pm 1.3 \times 10^{-8} \text{ cm}^2/\text{s}$. In some membranes, it took some time for the capacitance signal to rise to its equilibrium level (Fig. 3 A). In such cases there was a similar evolution of D with time. A somewhat smaller increase in D was still evident in cases where stable capacitance levels were achieved rapidly (Fig. 3 B), which was the case for most bilayers discussed in this paper.

The influence of properties of the septum in the PLB cell on the lateral diffusion coefficient was also studied. The monotonic increase in capacitance during the formation of the bilayer indicates that the bilayer reaches its equilibrium via a thinning process (Niles et al., 1988) and not according to a “locking-in” process (Brullemans and Tancrede, 1987; Schindler, 1989). The important parameter in this respect is the hole diameter:septum thickness ratio, which was in the range of 6 to 15 in most of our experiments. Some experiments were performed under conditions that favored the locking-in process using PLBs formed by using a $10\text{-}\mu\text{m}$ PTFE septum (ratio higher than 20) as the support. However, no significant change in the equilibrium value of D was observed (Table 1). Similarly, no significant change in either of these properties was observed in membranes formed from zwitterionic phospholipid mixtures (e.g., POPC:DOPE, 7:3) when the ionic strength of the suspending buffer was changed from 1 M to 100 mM KCl (Table 1).

The specific capacitances of the PLBs reported here were around $700 \text{ nF}/\text{cm}^2$, in good agreement with data obtained on virtually solvent-free bilayers formed from lipids with 18 carbon chains (Benz et al., 1975; Digler and Benz, 1985; White, 1986). They are also reasonable given the theoretical hydrophobic thickness of POPC:DOPE bilayers. The latter were chosen as our standard, because they have been widely used in reconstitution assays with alamethicin (Keller et al., 1993, modulation of channel behavior with the PE:PC ratio and the inverted hexagonal phase tendency), with natural and synthetic analogs (Rebuffat et al., 1992; Duclozier et al., 1992), and with model peptides for ion channels (Brullemans et al., 1994).

Phospholipid composition and lateral diffusion in PLBs

The influence of the molecular structure of the constituent phospholipids (POPC and DOPE) on D in PLBs was inves-

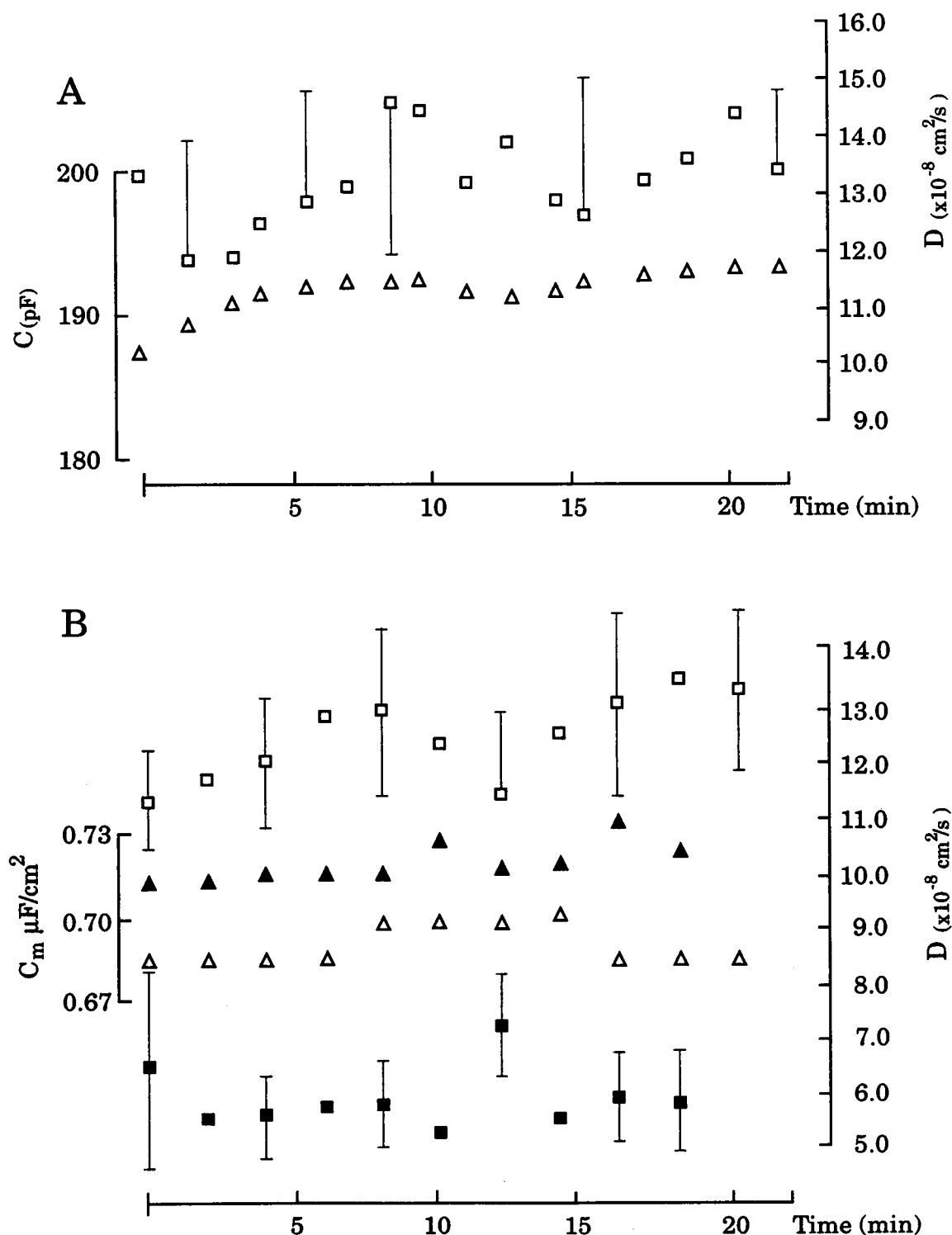


FIGURE 3 Lateral diffusion coefficient and membrane capacitance during the bilayer's lifespan. (A) Change in lateral diffusion (\square) and capacitance (Δ) of the POPC:DOPE (7:3) bilayer with time. (B) Change in lateral diffusion and specific capacitance of another POPC:DOPE (7:3) bilayer alone (lateral diffusion, \square ; specific capacitance, Δ) or containing equimolar cholesterol (lateral diffusion, \blacksquare ; specific capacitance, \blacktriangle) with time.

tigated. Specifically, the influence of unsaturation in the second aliphatic chain (DOPC versus POPC) and the chemical nature and electrical charge of the headgroups (DOPC versus DOPE and DOPS) was addressed. The results are

presented in Table 2 and show that the presence of the second unsaturated chain in DOPC does not significantly alter D from the value observed with POPC, in spite of the greater "kink effect" (Stubbs et al., 1981) that this imparts to

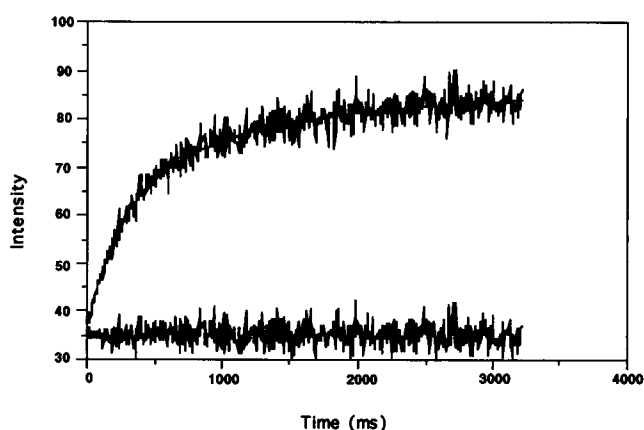


FIGURE 4 A typical recovery portion of a FRAP curve obtained from a "virtually solvent-free" planar bilayer formed from DOPC containing 1% (mole/mole) NBD-PE. The data were averaged and analyzed as described in the text. The smooth line is the computed fit to the data curve, and the residual (i.e., data minus fit) is also shown.

the fatty acid chains. Bilayers made of lipids favoring inverted hexagonal phase (PE) or negatively charged headgroups may exhibit slightly reduced lateral mobility.

Changes in D in PLBs as a function of cholesterol content

The addition of 10% or 20% cholesterol (molar ratio) to the POPC:DOPE (7:3) lipid solutions in hexane followed by PLB formation resulted in bilayers in which the lateral diffusion coefficient was slightly reduced from $13.3 \times 10^{-8} \text{ cm}^2/\text{s}$ to 11.9 and $11.8 \times 10^{-8} \text{ cm}^2/\text{s}$, respectively.

The amount of cholesterol present in the lipid solution had to be raised to 50% to yield an appreciable effect upon the lateral mobility of the NBD-PE lipid probe in the bilayer. Specifically, in the POPC:DOPE (7:3) lipid solutions, incorporation of 33% or 50% cholesterol (mole ratio) resulted in a reduction in D by a factor of 2. In bilayers formed from DOPC alone, the addition of similar levels of cholesterol reduced D from 13.4 to $8.9 \times 10^{-8} \text{ cm}^2/\text{s}$ (Table 3). No significantly different value for D was found when the probe was incorporated into the cholesterol-containing leaflet of the bilayer (asymmetric DOPC/CHOL bilayers; Table 3). This would suggest that cholesterol dominates the be-

TABLE 1 The effect of ionic strength of the bathing media and the PTFE film thickness on the lateral diffusion ($D \pm \text{SD}$) and percentage recovery ($\%R \pm \text{SD}$) in planar lipid bilayers

Bilayer composition	[KCl] (mM)	$D \times 10^8 \text{ (cm}^2/\text{s)}$ (% recovery)	$N(\text{det})$	$N(\text{PLB})$
POPC:DOPE (7:3)	1000	13.2 ± 1.07 (100.8 ± 2.0)	17	4
POPC:DOPE (7:3)	100	13.3 ± 0.8 (101.0 ± 0.9)	18	3
POPC:DOPE (7:3) (10 μm PTFE)	100	12.7 ± 0.69 (99.5 ± 3.0)	10	3

$N(\text{det})$, Number of determination of lateral diffusion; $N(\text{PLB})$, number of planar lipid bilayers.

TABLE 2 Influence of phospholipid structure on lateral diffusion ($D \pm \text{SD}$) and percentage recovery ($\%R \pm \text{SD}$) in planar lipid bilayers

Bilayer composition	[KCl] (mM)	$D \times 10^8 \text{ (cm}^2/\text{s)}$ (% recovery)	$N(\text{det})$	$N(\text{PLB})$
POPC	100	12.9 ± 1.2 (98.1 ± 5.6)	8	3
DOPC	100	13.4 ± 0.7 (101.5 ± 1.2)	13	3
DOPE	100	12.5 ± 1.4 (100.1 ± 1.9)	11	3
DOPS	100	12.4 ± 1.3 (100.2 ± 2.5)	18	7

$N(\text{det})$, Number of determination of lateral diffusion; $N(\text{PLB})$, number of planar lipid bilayers.

havior as far as lipid lateral diffusion is concerned. Nevertheless, it should be noted that this reflects the fact that the bilayer asymmetry is quite difficult to control experimentally and is likely to differ from one membrane to another. In all cases, even with ternary mixtures, the recovery is equal to 100%.

Effects of added calcium on lateral diffusion in PLBs formed from negatively charged lipids

We reported above that the lateral diffusion coefficient of NBD-PE in DOPS bilayers was essentially indistinguishable from that observed in bilayers formed from DOPE, i.e., lipids with the same acyl chain structure, length, and unsaturation, but bearing phosphatidylethanolamine headgroups), and D in these systems was slightly lower than that observed with DOPC (Table 2). In an effort to distinguish between diffusion behavior of the different headgroups, the effect of calcium on the chelation of negatively charged headgroups was investigated. The results shown in Table 4 reveal that D in DOPS bilayers was substantially reduced from 12.4 to $8.3 \times 10^{-8} \text{ cm}^2/\text{s}$ when either 150 or 15 mM CaCl_2 was added to the bathing medium. Even when the calcium concentration was reduced a further 10-fold to 1.5 mM, the effect was still saturating. It is notable that the percentage recovery ($\%R$) was still around 100% in the pure phospholipid and phospholipid plus cholesterol studies.

Influence of the incorporation of the pore-former alamethicin into PLBs

The effect of the addition of alamethicin, a 20-residue peptide isolated from *Trichoderma viride* and well known for its ability to develop highly voltage-dependent conductances in such bilayers (Boheim, 1974; Hall et al., 1984), on POPC:DOPE PLBs was investigated. The addition of $3.4 \times 10^{-8} \text{ M}$ alamethicin (from a 10^{-5} M stock solution in methanol) to the *cis* side (1 M KCl) of the chamber led to both the development of the characteristic macroscopic current-voltage curve under appropriate voltage ramp conditions (Fig. 5) and to a small but significant reduction in D . Specifically, at 0 mV, D was reduced from 13.8 ± 1.0 to $11.1 \pm 0.8 \times 10^{-8} \text{ cm}^2/\text{s}$ ($N = 3$). The specific bilayer

TABLE 3 Influence of cholesterol content on lateral diffusion ($D \pm SD$) and percentage recovery ($\%R \pm SD$) in planar lipid bilayers

Bilayer composition		[KCl] (mM)	$D \times 10^8$ (cm ² /s) (% recovery)	N(det)	N(PLB)
<i>Cis</i> side	<i>Trans</i> side				
POPC:DOPE (7:3)	POPC:DOPE (7:3)	100	13.3 \pm 0.8 (101.0 \pm 0.9)	18	3
POPC:DOPE:CHOL (7:3:5)	POPC:DOPE:CHOL (7:3:5)	100	6.2 \pm 0.6 (98.0 \pm 1.6)	16	3
POPC:DOPE:CHOL (7:3:10)	POPC:DOPE:CHOL (7:3:10)	100	6.2 \pm 0.6 (101.4 \pm 2.2)	16	3
DOPC	DOPC	100	13.4 \pm 0.7 (101.5 \pm 1.2)	13	3
DOPC:CHOL (1:1)	DOPC:CHOL (1:1)	100	8.9 \pm 1.1 (101.2 \pm 1.2)	16	3
CHOL + probe	DOPC	100	9.6 \pm 3.5 (101.5 \pm 0.5)	4	2

N(det), Number of determination of lateral diffusion; N(PLB), number of planar lipid bilayers.

capacitance was little affected (0.76 versus 0.79 $\mu\text{F}/\text{cm}^2$) by the incorporation of alamethicin.

DISCUSSION

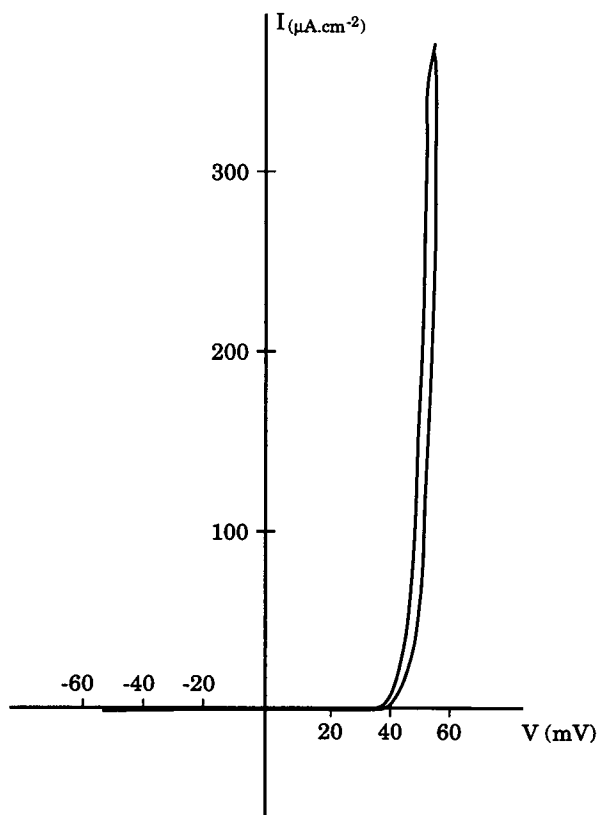
The principal objective of this paper was to report the construction and operation of an apparatus that allows formation and investigation of PLBs by simultaneous observation of membrane integrity and permeability through capacitance and conductance measurements and lipid mobility by measurement of lateral diffusion by FRAP on the same membrane (PLB). The data presented represent the first reliable measurements of lipid lateral diffusion, under a range of chemical conditions (albeit nonexhaustive) in conventional (i.e., "nonsupported") planar bilayers. They demonstrate the feasibility of the FRAP approach to systems mostly widely used in the electrical characterization of transmembrane transport of ions. Furthermore, both kinds of measurements can be combined simultaneously on the same bilayer, offering an integrated view of the membrane dynamics and function interrelations. The approach we present has considerable scope for application in structure-function studies of membrane-associating molecules such as porins and other channel-forming proteins, or peptides such as alamethicin, the voltage-dependent aggregation of which is brought about after some monomer lateral diffusion; antimicrobial molecules such as nisin; and surface-active dietary components such as saponins.

TABLE 4 The effect of calcium ions on lateral diffusion ($D \pm SD$) and percentage recovery ($\%R \pm SD$) in negatively-charged planar lipid bilayers

Bilayer composition and divalent cations	[KCl] (mM)	$D \times 10^8$ (cm ² /s) (% recovery)	N(det)	N(PLB)
DOPS	100	12.4 \pm 1.3 (100.2 \pm 2.5)	18	7
DOPS + CaCl ₂ (1.5 mM)	100	5.9 \pm 0.25 (105.0 \pm 1.8)	3	2
DOPS + CaCl ₂ (15 mM)	100	8.4 \pm 1.2 (100.9 \pm 3.5)	6	2
DOPS + CaCl ₂ (150 mM)	100	8.3 \pm 1.2 (100.1 \pm 4.5)	17	6

N(det), Number of determination of lateral diffusion; N(PLB), number of planar lipid bilayers.

Formation of planar membranes by the Montal-Mueller method was achieved, and their evolution with time was monitored by capacitance measurements. The equilibrium and average value of 0.7 $\mu\text{F}/\text{cm}^2$ reported here could be converted in terms of dielectric thickness, using the parallel-plate capacitor model with a dielectric permittivity of 2.2 (for oleic acid). The hydrocarbon core thickness we obtained (2.78 nm) compares well with x-ray diffraction measurements on DOPC (Lewis and Engleman, 1983) and suggests that the dielectric boundary is near the acetyl region. White (1977) estimated that the minimum hydrocarbon thickness of glycerol monooleate bilayers to be 2.5 nm. No

**FIGURE 5** Macroscopic current-voltage curves for POPC:DOPE (7:3) bilayer after equilibration with 3.4×10^{-8} M alamethicin in the *cis* side (1 M KCl)

such analysis is available for phospholipids, but values of $0.75 \mu\text{F}/\text{cm}^2$ have been reported for dioleoyl-phospholipid bilayers (Brullemans and Tancrede, 1987). Thus it seems that the bilayers studied here are quasi-solvent-free.

We have demonstrated that it is possible to conduct simultaneous measurements of the lateral diffusion of a fluorescently labeled phospholipid analog, NBD-PE, in these planar lipid membranes over the same time course. This has an additional benefit, because as the determinations of D are subject to significant errors (standard deviations typically $\pm 10\%$), collecting the data over a long period allows an average D value to be estimated. The lateral diffusion coefficient obtained on Montal-Mueller bilayers for a range of unsaturated phospholipids ($\sim 13 \pm 1 \times 10^{-8} \text{ cm}^2/\text{s}$) compares favorably with published data on supported bilayers formed on electron microscopy grids. The diffusion of fluorophores in the latter membranes was measured by fluorescence correlation spectroscopy and yielded D values of $17 \pm 2 \times 10^{-8} \text{ cm}^2/\text{s}$ (Fahey et al., 1977). Good agreement is also found with previous FRAP determinations of D in large egg PC vesicles with reported values of $12 \times 10^{-8} \text{ cm}^2/\text{s}$ at 24°C (Fahey and Webb, 1978). In contrast, results obtained from Langmuir-Blodgett bilayers are systematically lower (Tamm and McConnell, 1985). As the same applies for POPC multilayer films deposited on solid substrates (Pearce et al., 1992), it is likely that lateral diffusion in such systems is hindered by the minute hydration layers. As for cell membranes, D values obtained using fluorescent lipid analogs are in the range 0.01 to $1 \times 10^{-8} \text{ cm}^2/\text{s}$, reflecting the restraining effect of both cytoskeleton and protein aggregates on the probe mobility (Greenberg and Axelrod, 1993; Ladha et al., 1994).

The data also show good agreement with our own observations of lateral diffusion of 5-*N*-octadecanoyl amino fluorescein in thick (88 nm) equilibrium phospholipid-stabilized foam films (Lalchev et al., 1994, 1995), in which the orientation of the lipid molecules is the inverse of that in the PLBs. It is interesting to compare both sets of studies, because this allows consideration of the effect of the phospholipid headgroup in determining D . In the present study, no significant difference was observed between D of NBD-PE in negatively charged PS bilayers and in zwitterionic bilayers formed from PC or PE. This is perhaps a little surprising, because PE headgroups are capable of hydrogen bonding. In contrast, studies performed on common black and Newton black foam films (typically 12 nm and 6 nm thick, respectively) showed that lateral diffusion of lipid analogs was acutely sensitive to the predominant headgroup type (Lalchev et al., 1994). The temperature dependence of D of a lipid analog in foam films formed from synthetic saturated phospholipids was systematically studied in the latter paper. Unfortunately, such lipids do not form stable planar membranes, so direct comparison was limited to comparable measurements on both systems using DOPE. The observed D in common black foam films of DOPE at 23°C was $2.5 \times 10^{-8} \text{ cm}^2/\text{s}$ (Lalchev et al., 1994). This is approximately fivefold less than that observed in PLBs. It

would be useful to examine POPC, DOPC, and DOPS in the foam film system and to extend the PLB studies across a range of temperatures to extend comparisons. Nevertheless, the existing data support the view that the orientation of the lipid molecules in the PLB results in an electrically insulating layer that eliminates headgroup-headgroup interactions but favors frictional drag between lipids in different leaflets of the PLBs. Our PLB results, and particularly the lack of any significant modulation of D by different headgroups, also contrast with molecular dynamics simulation studies of lipid bilayer fluidity, which conclude that the "apparent high viscosity of the membrane is more closely related to molecular interactions on the surface rather than in the interior" (Venables et al., 1993).

However, other factors did induce changes in lipid diffusion in Montal-Mueller conventional bilayers. The well-documented membrane-stiffening effect of cholesterol on fluid phases (Presti, 1985) was also detected in our model membranes (Table 3). Comparable effects of cholesterol have previously been reported: the decrease in D from 5 to $4 \times 10^{-8} \text{ cm}^2/\text{s}$ for DOPE multilamellar vesicles containing 10% cholesterol (Chen et al., 1990), the decrease from 3.5 to $2.5 \times 10^{-8} \text{ cm}^2/\text{s}$ of POPC multilamellar vesicles containing 20% cholesterol (Shin and Freed, 1989), and the decrease from 4 to $2 \times 10^{-8} \text{ cm}^2/\text{s}$ for egg PC multilayers containing 50% cholesterol (Wu et al., 1977). The variation of D with cholesterol concentration obtained with our DOPC bilayers complements the results by Hianik et al. (1984) on the viscosity of egg PC black films and those by Chang et al. (1995) on the mean open time and conductance of the BK channel in POPE-POPS black films. Future experiments should nevertheless be performed to determine whether a minimum of D is present between 20% and 33%. We have also detected a significant variation in D with calcium concentration for DOPS bilayers, but in contrast to the cholesterol effects, few data are available in the literature for comparison. Key reports in this respect were published by Blatt and Vaz (1986), who identified some reduction in D for DMPC multilayers in the presence of calcium, and recently by Schootemeijer et al. (1994), showing in human megakaryoblastic cells a reduction in D from $3.5 \times 10^{-9} \text{ cm}^2/\text{s}$ to $2.9 \times 10^{-9} \text{ cm}^2/\text{s}$ in the presence of 0.4 mM calcium. The biological implications of divalent cation effects on membrane dynamics are potentially far-reaching in signal transduction pathways involving fast and localized surges of calcium concentrations near the inner leaflet of the membrane, which is richer in negatively charged phospholipid than the outer leaflet.

As for the effect of the addition of the pore-former alamethicin, it is consistent with the idea that obstacles within the bilayer would reduce the mean coefficient of lipid lateral diffusion (Schram et al., 1994). Any quantitative appreciation of this effect requires first an estimation, from the literature, of the fraction of the bilayer area covered by alamethicin. Extrapolating the binding curves obtained by Cafiso and co-workers with a spin-labeled alamethicin derivative (Cafiso, 1994) and POPC/POPE (7/3), a

lipid mixture close to the one used in the present work, the alamethicin aqueous concentration we used (35 nM) would correspond to a peptide/lipid ratio (P/L) of $\sim 1:2000$. From the absorption isotherm of alamethicin at the interface between glycerol monooleate and 1 M NaCl (Gordon and Haydon, 1975), still extrapolated to 35 nM, about 5×10^9 peptide molecules would be absorbed per mm^2 , i.e., $P/L \approx 1:300$. This figure is comparable with a more direct estimation given by Fringeli (1980), P/L [dim] 1:550 for 28 nM alamethicin in equilibrium with saturated lipids and using infrared spectroscopy.

Another parameter to consider is of course the orientation of alamethicin at the water-lipid interface, because the membrane area occupied by an alamethicin molecule (equivalent to a 20-residue helix) will be either roughly 2 or 4.5 nm^2 , depending on which orientation (perpendicular or parallel to the bilayer) is preferred. This orientation was shown to be dependent upon the lipid hydration and the alamethicin aqueous concentration (Huang and Wu, 1991). Under the conditions used here, which are compatible for conductance measurements, the peptide is assumed to be mostly perpendicular to the bilayer surface. Taking into account the P/L range estimated above, which is well below what would be needed to induce the hexagonal H_{II} lipid phase (see, e.g., Batenburg et al., 1987, for melittin with cardiolipin), with presumably an anomalous lateral diffusion, the fraction of bilayer area to be covered by alamethicin may thus be in the 0.5–1% range.

This, associated with the 20% reduction in D , will then be more compatible with theoretical predictions assuming relatively immobile obstacles rather than with mobile obstacles. As shown by Bussell et al. (1995), with a model considering both "short-time hydrodynamic and long-time thermodynamic interactions," a fractional area of 1% covered by immobile obstacles reduces D by almost 20%. The predicted values are about one decade less than those reported here, the system being quite different (surface immunoglobulins in mouse lymphocytes), but the form of their theoretical curve remains the same for hydrodynamic conditions similar to ours. In addition, a significant alamethicin fraction lying flat on the bilayer or some preaggregates, even for no voltage applied, could contribute to the observed decrease in D .

CONCLUSIONS AND PERSPECTIVES

An apparatus has been described that allows the simultaneous measurement of lateral diffusion by FRAP and the evaluation of membrane integrity by capacitance and conductance monitoring. Experiments performed on membranes composed of individual or mixed synthetic phospholipids have validated the method and shown that lipid diffusion is insensitive to headgroup type but significantly altered in the presence of added cholesterol or calcium. The method offers opportunities for systematic studies of lipid bilayers. In particular, the method offers real opportunities

in the investigation of structure-function relationships in membranes by combining spectroscopic and electrical recording techniques, as suggested recently (MacDonald and Wraight, 1995).

Investigations are in progress to establish the relationship between applied voltage and lateral diffusion of lipids in planar lipid bilayers. To address the important question of the effect of applied voltage on alamethicin diffusion, a fluorescein-labeled alamethicin analog is being synthesized and its conductance properties described (Dugast et al., manuscript in preparation). This fluorescent alamethicin analog will be used to resolve the different diffusion regimes associated with the sizes of the conducting aggregates that are postulated in the "barrel-stave" model.

Supported by a Franco-British Alliance Programme. MB acknowledges the NSERC (Canada) for a postdoctoral fellowship. SL, ARM, LJH, and DCC were supported by OST funding from the BBSRC.

REFERENCES

- Anderson, C. M., G. N. Georgiou, I. E. G. Morrison, G. V. W. Stevenson, and R. J. Cherry. 1992. Tracking of cell surface receptors by fluorescence digital imaging microscopy using a charge coupled device camera—low density lipoprotein and influenza virus receptor mobility at 4°C . *J. Cell Sci.* 101:415–425.
- Batenburg, A. M., J. C. L. Hibbeln, A. J. Verkleij, and B. de Kruijff. 1987. Melittin induces H-II phase formation in cardiolipin model membranes. *Biochim. Biophys. Acta.* 903:142–154.
- Benz, R., O. Fröhlich, P. Läger, and M. Montal. 1975. Electrical capacity of black lipid films and of lipid bilayers made from monolayers. *Biochim. Biophys. Acta.* 394:323–334.
- Blackwell, M., C. Gubas, S. Gyga, D. Roman, and B. Wagner. 1994. The plastoquinone diffusion coefficient in chloroplasts and its mechanistic implications. *Biochim. Biophys. Acta.* 1183:553–543.
- Blatt, E., and W. L. C. Vaz. 1986. The effects of Ca^{++} on lipid diffusion. *Chem. Phys. Lipids.* 41:183–194.
- Bloom, J. A., and W. W. Webb. 1983. Lipid diffusibility in the intact erythrocyte membrane. *Biophys. J.* 42:295–305.
- Boheim, G. 1974. Statistical analysis of alamethicin channels in black membranes. *J. Membr. Biol.* 19:277–303.
- Brullemans, M., O. Helluin, I. Y. Dugast, G. Molle, and H. Duclouier. 1994. Implication of segment S_{45} in the formation pathway of voltage-dependent sodium channels. *Eur. Biophys. J.* 23:39–40.
- Brullemans, M., and P. Tancrede. 1987. Influence of torus on the capacitance of asymmetrical phospholipid bilayers. *Biophys. Chem.* 27:225–231.
- Bussell, S. J., D. L. Koch, and D. A. Hammer. 1995. Effect of hydrodynamic interactions on the diffusion of integral membrane proteins: diffusion in plasma membranes. *Biophys. J.* 68:1836–1849.
- Cafiso, D. S. 1994. Alamethicin: a peptide model for voltage gating and protein-membrane interactions. *Annu. Rev. Biophys. Biomol. Struct.* 23:141–165.
- Chang, H. M., R. Reitsjeter, R. P. Mason, and R. Gruener. 1995. Attenuation of excimer kinetics and conductance by cholesterol: an interpretation using structural stress as a unifying concept. *J. Membr. Biol.* 143:51–63.
- Chen, S. Y., K. H. Cheng, and D. M. Ortano. 1990. Lateral diffusion study of excimer-forming lipids in lamellar to inverted hexagonal phase-transition of unsaturated phosphatidylethanolamine. *Chem. Phys. Lipids.* 53:321–329.
- Cherry, R. J., G. N. Georgiou, and I. E. G. Morrison. 1994. New insights into the structure of cell membranes from single particle tracking experiments. *Biochem. Soc. Trans.* 22:781–784.

- Clark, D. C. 1995. Application of state-of-the-art fluorescence and interferometric techniques to study coalescence in food dispersions. In *Characterisation of Food: Emerging Methods*. A. Gaonkar, editor. Elsevier, Amsterdam. 23–57.
- Clark, D. C., R. Dann, A. R. Mackie, J. Mingins, A. C. Pinder, P. W. Purdy, E. J. Russell, L. J. Smith, and D. R. Wilson. 1990. Surface diffusion in SDS stabilized thin liquid films. *J. Colloid Interface Sci.* 138:195–206.
- Cossins, A. R. 1983. The adaptation of membrane structure and function to changes in temperature. In *Cellular Adaptation to Environmental Changes*. A. R. Cossins and P. Shetlerline, editors. Cambridge University Press, Cambridge, London, New York. 3–32.
- Cuculescu, M., D. Hyde, and K. Bowler. 1995. Temperature acclimation of marine crabs: changes in plasma membrane fluidity and lipid composition. *J. Therm. Biol.* 20:207–222.
- Davoust, J., P. F. Devaux, and L. Leger. 1982. Fringe pattern photobleaching, a new method for the measurement of transport coefficients of biological macromolecules. *EMBO J.* 1:1233–1238.
- Digler, J. P., and R. Benz. 1985. Optical and electrical-properties of thin monoolein lipid bilayers. *J. Membr. Biol.* 85:181–189.
- Duclohier, H., G. Molle, J. Y. Dugast, and G. Spach. 1992. Prolines are not essential residues in the "barrel-stave" model for ion channels induced by alamethicin analogues. *Biophys. J.* 63:868–873.
- Fahey, P. F., D. E. Koppel, L. S. Barak, D. E. Wolf, E. L. Elson, and W. W. Webb. 1977. Lateral diffusion in planar lipid bilayers. *Science*. 195:305–306.
- Fahey, P. F., and W. W. Webb. 1978. Lateral diffusion in phospholipid bilayer membranes and multilamellar liquid crystals. *Biochemistry*. 17:3046–3053.
- Fringeli, U. P. 1980. Distribution and diffusion of alamethicin in a lecithin/water model membrane system. *J. Membr. Biol.* 54:203–212.
- Gordon, L. G. M., and D. A. Haydon. 1975. Potential-dependent conductances in lipid membranes containing alamethicin. *Phil. Trans. R. Soc. Lond. B.* 270:433–447.
- Greenberg, M., and D. Axelrod. 1993. Anomalous slow mobility of fluorescent lipid probes in the plasma membrane of the yeast *Saccharomyces cerevisiae*. *J. Membr. Biol.* 131:115–127.
- Hall, J. E., G. R. Marshall, and I. Vodyanoy. 1984. Alamethicin as a model for voltage-gated ion channels. *Biophys. J.* 45:233–247.
- Hanke, W., and W. R. Schlue. 1993. Planar Lipid Bilayers. Methods and Applications. Academic Press, London, San Diego.
- Hianik, T., P. Kvasnicka, and K. Strofferova. 1984. Mechanical properties of lipid bilayers with varying cholesterol content. *Stud. Biophys.* 100:23–32.
- Huang, H. W., and Y. Wu. 1991. Lipid-alamethicin interactions influence alamethicin orientation. *Biophys. J.* 60:1079–1087.
- Jacobson, K., E. R. Sheets, and R. Simpson. 1995. Revisiting the fluid mosaic model. *Science*. 268:1441–1442.
- Joe, E. H., and K. J. Angelides. 1993. Clustering and mobility of voltage-dependent sodium channels during myelination. *J. Neurosci.* 13:2993–3005.
- Keller, S. L., S. M. Bezrukov, S. M. Gruner, M. W. Tate, I. Vodyanoy, and V. A. Parsegian. 1993. Probability of alamethicin conductance states varies with nonlamellar tendency of bilayer phospholipids. *Biophys. J.* 65:23–27.
- Koppel, D. E., D. Axelrod, J. Schlessinger, E. L. Elson, and W. W. Webb. 1976. Dynamics of fluorescence marker concentration as a probe of mobility. *Biophys. J.* 16:1315–1329.
- Krueger, B. K., J. F. Worley, and R. J. French. 1983. Single sodium channel from rat brain incorporated into planar lipid bilayers. *Nature*. 303:172–175.
- Ladha, S., A. R. Mackie, and D. C. Clark. 1994. Cheek cell membrane fluidity measured by fluorescence recovery after photobleaching and steady state anisotropy. *J. Membr. Biol.* 142:223–229.
- Lalchev, Z. I., P. J. Wilde, and D. C. Clark. 1994. Surface diffusion in phospholipid foam films. 1. Dependence of the diffusion coefficient on the lipid phase state, molecular length, and charge. *J. Colloid Interface Sci.* 167:80–86.
- Lalchev, Z. I., P. J. Wilde, A. R. Mackie, and D. C. Clark. 1995. Surface diffusion on phospholipid foam films. 2. The effect of film type, and temperature cycling on surface diffusion. *J. Colloid Interface Sci.* 174:283–288.
- Lamb, T. D. 1994. Stochastic simulation of activation in the G-protein cascade of phototransduction. *Biophys. J.* 67:1439–1454.
- Leckband, D. E., J. N. Israelachvili, F. J. Schmitt, and W. Knoll. 1992. Long-range attraction and molecular-rearrangements in receptor-ligand interactions. *Science*. 255:1419–1421.
- Lewis, B. A., and D. M. Engelman. 1983. Lipid bilayer thickness varies linearly with acyl chain length in fluid phosphatidylcholine vesicles. *J. Mol. Biol.* 166:211–217.
- MacDonald, A. G., and P. C. Wraight. 1995. Combined spectroscopic and electrical recording techniques in membrane research: prospects for single channel studies. *Prog. Biophys. Mol. Biol.* 63:1–29.
- Montal, M., and P. Mueller. 1972. Formation of bimolecular membranes from monolayers and study of their properties. *Proc. Natl. Acad. Sci. USA*. 69:3561–3566.
- Niles, W. D., R. A. Levis, and F. S. Cohen. 1988. Planar bilayer membranes made from phospholipid monolayers formed by a thinning process. *Biophys. J.* 53:327–335.
- Pearce, K. H., R. G. Hiskey, and N. L. Thompson. 1992. Surface binding kinetics of prothrombin fragment 1 on planar membranes measured by total internal reflection fluorescence microscopy. *Biochemistry*. 31:5983–5995.
- Presti, F. T. 1985. The role of cholesterol in regulating membrane fluidity. In *Membrane Fluidity in Biology*, Vol. 4. R. C. Aloia and J. M. Boggs, editors. Academic Press, New York. 97–146.
- Rebuffat, S., H. Duclohier, C. Auvin-Guette, G. Molle, G. Spach, and B. Bodo. 1992. Membrane-modifying properties of the pore-forming peptides satumsporin SA IV and harzianin HA V. *FEMS Microbiol. Immunol.* 105:151–160.
- Schindler, H. 1989. Planar lipid-protein membranes: strategies of formation and of detecting dependencies of ion transport functions on membrane conditions. *Methods Enzymol.* 171:225–253.
- Schlessinger, J. 1993. Lateral and rotational diffusion of EGF-receptor complex relationship to receptor mediated endocytosis. *Biopolymers*. 22:47–353.
- Schootemeijer, A., A. E. Van Beekhuizen, L. G. J. Tertoolen, S. W. De Laat, and J. W. N. Akkerman. 1994. Cytosolic calcium ions regulate lipid mobility in the plasma membrane of the human megakaryoblastic cell line MEG-O1. *Eur. J. Biochem.* 224:423–430.
- Schram, V., J. F. Tocanne, and A. Lopez. 1994. Influence of obstacles on lipid lateral diffusion: computer simulations of FRAP experiments and application to proteoliposomes and biomembranes. *Eur. Biophys. J.* 23:337–348.
- Shin, Y. K., and J. H. Freed. 1989. Thermodynamics of phosphatidylcholine-cholesterol mixed model membranes in the liquid crystalline state studied by the orientational order parameter. *Biophys. J.* 56:1093–1100.
- Shinitzky, M. 1984a. Membrane fluidity and cellular functions. In *Physiology of Membrane Fluidity*, Vol. 1. M. Shinitzky, editor. CRC Press, Boca Raton, FL. 1–51.
- Shinitzky, M. 1984b. Membrane fluidity in malignancy: adversative and recuperative. *Biochim. Biophys. Acta*. 738:251–261.
- Smith, B. A., and H. M. McConnell. 1978. Determination of molecular motion in membranes using periodic pattern photobleaching. *Proc. Natl. Acad. Sci. USA*. 75:2759–2763.
- Stubbs, C. D., T. Kouyama, K. Kinoshita, and A. Ikegami. 1981. Effect of double bonds on the dynamic properties of the hydrocarbon region of lecithin bilayers. *Biochemistry*. 20:4257–4262.
- Tamm, L. K., and H. M. McConnell. 1985. Supported phospholipid bilayers. *Biophys. J.* 47:105–113.
- Tocanne, J. F., L. Dupou-Cézanne, and A. Lopez. 1994. Lateral diffusion of lipids in model and natural membranes. *Prog. Lipid Res.* 33:203–237.
- Tournier, J. F., A. Lopez, N. Gas, and J. F. Tocanne. 1989. The lateral motion in the apical plasma membrane of endothelial cells is reversibly affected by the presence of cell junctions. *Exp. Cell Res.* 181:375–384.
- Venables, R. M., Y. Zhang, B. J. Hardy, and R. W. Pastor. 1993. Molecular dynamics simulations of a lipid bilayer and of hexadecane: an investigation of membrane fluidity. *Science*. 262:223–226.
- Vodyanoy, V., and R. B. Murphy. 1982. Solvent-free lipid bimolecular membranes of large surface area. *Biochim. Biophys. Acta*. 687:189–194.

- Wedekind, P., U. Kubitschek, and R. Peters. 1994. Scanning microphotolysis: a new photobleaching technique based on fast intensity modulation of a scanned laser beam and confocal imaging. *J. Microsc.* 176:23–33.
- White, S. H. 1977. Studies of the physical chemistry of planar bilayer membranes using high-precision measurements of specific capacitance. *Ann. N.Y. Acad. Sci.* 303:243–265.
- White, S. H. 1986. The physical nature of planar bilayer membranes. In *Ion Channel Reconstitution*. C. Miller, editor. Plenum Press, New York. 3–35.
- Wolf, D. E. 1989. Designing, building and using a fluorescence recovery after photobleaching instrument. *Methods Cell Biol.* 30:271–306.
- Wu, E. D., D. W. Tank, and W. W. Webb. 1977. Lateral diffusion in phospholipid multibilayers measured by fluorescence recovery after photobleaching. *Biochemistry.* 16:3936–3941.
- Yguerabide, J., J. A. Schmidt, and E. E. Yguerabide. 1982. Lateral mobility in membranes as detected by fluorescence recovery after photobleaching. *Biophys. J.* 39:69–75.